

## Errata and Addenda: Theory of Dielectric Relaxation for a Single-Axis Rotator in a Crystalline Field

John D. Hoffman

Citation: [The Journal of Chemical Physics](#) **22**, 1144 (1954); doi: 10.1063/1.1740298

View online: <http://dx.doi.org/10.1063/1.1740298>

View Table of Contents: <http://scitation.aip.org/content/aip/journal/jcp/22/6?ver=pdfcov>

Published by the [AIP Publishing](#)

---

### Articles you may be interested in

[Temperature dependence of single-axis acoustic levitation](#)

J. Appl. Phys. **93**, 3016 (2003); 10.1063/1.1540232

[Parametric study of single-axis acoustic levitation](#)

Appl. Phys. Lett. **79**, 881 (2001); 10.1063/1.1391398

[Theory of Dielectric Relaxation for a Single-Axis Rotator in a Crystalline Field. II](#)

J. Chem. Phys. **23**, 1331 (1955); 10.1063/1.1742270

[Calculation of the Distribution of Relaxation Times for a Single-Axis Rotator Using the Random-Jump Hypothesis](#)

J. Chem. Phys. **22**, 156 (1954); 10.1063/1.1739845

[Theory of Dielectric Relaxation for a Single-Axis Rotator in a Crystalline Field](#)

J. Chem. Phys. **22**, 132 (1954); 10.1063/1.1739821

---

A promotional banner for AIP Applied Physics Reviews. On the left is a thumbnail of a journal cover for 'AIP Applied Physics Reviews' featuring a diagram of a device. The main part of the banner has a blue background with a bright light source and the text 'NEW Special Topic Sections' in large white letters. Below this, in an orange bar, it says 'NOW ONLINE' in yellow, followed by 'Lithium Niobate Properties and Applications: Reviews of Emerging Trends' in white. The AIP Applied Physics Reviews logo is in the bottom right corner of the orange bar.

**NEW Special Topic Sections**

**NOW ONLINE**  
Lithium Niobate Properties and Applications:  
Reviews of Emerging Trends

**AIP** Applied Physics Reviews

structure of the liquid and the following hindering of the rotations. Owing to the orienting field, the molecules execute angular oscillations about the direction of the field at a frequency much greater than the Larmor frequency. At Larmor frequency the rotation spectrum must therefore result less intense than Debye's theory would predict. We must think that in a liquid in which the hindrance potential is somewhat greater than  $kT$  the intensity of the rotation spectrum at Larmor frequency is determined by fluctuations in direction of the orienting field.

A description of the apparatus used and other results on nuclear relaxation in liquids will soon appear in *Il Nuovo Cimento*.

<sup>1</sup> Bloembergen, Purcell, and Pound, *Phys. Rev.* **73**, 679 (1948).

<sup>2</sup> N. Bloembergen, *Nuclear Magnetic Relaxation* (The Hague, 1948).

<sup>3</sup> G. Chiarotti and L. Giulotto, *Phys. Rev.* **93**, 1241 (1954).

## The Microwave Spectrum of Fluorobenzene\*

K. E. McCULLOH AND GILBERT F. POLLNOW

Department of Chemistry, State University of Iowa, Iowa City, Iowa

(Received April 2, 1954)

INVESTIGATION of the microwave spectrum of fluorobenzene was in progress at this laboratory when Erlandsson's report<sup>1</sup> of observation and interpretation of this spectrum became available to the authors. Frequency measurements in the present study were carried out to an accuracy of  $\pm 0.1$  mc, the results in most cases falling within Erlandsson's stated limits of error,  $\pm 5$  mc. This investigation confirms Erlandsson's assignment of frequencies and his proposed values for the rotational constants  $b$  and  $c$ , but a significantly different value is obtained for the parameter  $a$ .

Assignable absorption frequencies of fluorobenzene in the region 22.1–27.3 kmc were measured to  $\pm 0.1$  mc with the recording spectrometer<sup>2</sup> in use at the State University of Iowa. Of the 148 observed absorption lines, only those which have been assigned to specific rotational transitions are herein reported (see Table I).

TABLE I. Microwave frequencies of fluorobenzene.

Transition	Observed frequency	Calculated frequency
4 <sub>21</sub> –5 <sub>22</sub>	22322.2 mc	22322.0 mc
5 <sub>16</sub> –6 <sub>16</sub>	22863.5	22863.3
4 <sub>13</sub> –5 <sub>14</sub>	22940.9	22940.8
5 <sub>06</sub> –6 <sub>06</sub>	23134.7	23134.7
4 <sub>22</sub> –5 <sub>23</sub>	23393.8	23393.6
5 <sub>24</sub> –6 <sub>25</sub>	25427.4	25427.6
5 <sub>11</sub> –6 <sub>12</sub>	26378.8 <sup>a</sup>	26378.3
5 <sub>00</sub> –6 <sub>01</sub>	26378.8 <sup>a</sup>	26379.4
5 <sub>13</sub> –6 <sub>14</sub>	26445.2	26445.3
6 <sub>16</sub> –7 <sub>17</sub>	26460.7	26460.9
5 <sub>42</sub> –6 <sub>43</sub>	26483.2	26483.1
5 <sub>41</sub> –6 <sub>42</sub>	26528.9 <sup>b</sup>	26529.5
6 <sub>06</sub> –7 <sub>07</sub>	26605.3	26605.5
5 <sub>14</sub> –6 <sub>15</sub>	26960.2	26960.4
5 <sub>22</sub> –6 <sub>23</sub>	27163.3	27163.5

<sup>a</sup> Unresolved because of low intensities.

<sup>b</sup> Value uncertain because of broad line peak.

Observed intensities are consistent with the nuclear spin statistical weights of 10 for even  $K_{-1}$  and 6 for odd  $K_{-1}$ . In the computation of molecular constants (listed in Table II), reduced energies ob-

TABLE II. Molecular constants of fluorobenzene.

$\kappa = -0.58790 \pm 0.00002$
$(a-c)/2 = 1947.91$ mc
$(a+c)/2 = 3715.85$ mc
$I_a = 89.248$ amu A <sup>2</sup>
$I_b = 196.63$ amu A <sup>2</sup>
$I_c = 285.92$ amu A <sup>2</sup>
$I_c - I_a - I_b = 0.04$ amu A <sup>2</sup>

tained by the continued-fraction method<sup>3</sup> were employed throughout. No attempt was made to account for the effects of centrifugal distortion.

The experimentally determined moments of inertia and the observed dependence of line intensities upon the parity of  $K_{-1}$  lead to the conclusion that the molecule has a planar  $C_{2v}$  configuration. In order to examine the structure in more detail, the simplifying assumptions were made that the aromatic ring is a regular hexagon and that the HCC angles are  $120^\circ$ . An estimated value of 1.08 Å was assigned to the C–H distance. The interatomic distances obtained on this basis from the observed moments  $I_a$  and  $I_b$  are 1.40 Å for C–C (0.01 Å greater than Erlandsson's value) and 1.29 Å for C–F (Erlandsson gives 1.348 Å). Although it is difficult to appraise the reliability of the above-stated assumptions, it is interesting to note that Stoicheff's recent investigation<sup>4</sup> of the rotational Raman spectrum of benzene has yielded a value for  $I_a$  which is only 0.3 amu Å<sup>2</sup> lower than the corresponding moment of fluorobenzene as found in the present study.

\* Work supported by the U. S. Office of Naval Research.

<sup>1</sup> G. Erlandsson, *Arkiv Fysik* **6**, 477 (1953).

<sup>2</sup> G. W. Robinson, *J. Chem. Phys.* **21**, 1741 (1953).

<sup>3</sup> King, Hainer, and Cross, *J. Chem. Phys.* **11**, 27 (1943).

<sup>4</sup> B. Stoicheff, *J. Chem. Phys.* **21**, 1410 (1953).

## Errata and Addenda: Theory of Dielectric Relaxation for a Single-Axis Rotator in a Crystalline Field

[*J. Chem. Phys.* **22**, 132–141 (1954)]

JOHN D. HOFFMAN

National Bureau of Standards, Washington, D. C.

(Received April 5, 1954)

IN a recent issue<sup>1</sup> of this Journal a theory was given which described the distribution of dielectric relaxation times associated with a single-axis polar rotator in a crystalline field. This work included a calculation of the polarizability associated with each relaxation time. Although the polarizabilities quoted in the paper were correct, the description of the calculations was overly brief. Therefore, some relevant details are given in the following. This opportunity is also taken to correct some minor misprints, and to mention work now in progress.

The general method by which the polarizability value associated with a given relaxation time was obtained for a model with a given number of sites is illustrated for mode 2, i.e., we calculate the  $\alpha_2$  which appears with  $\tau_2$ .

(1) First, the polarization associated with each site [the coefficients of  $\psi_2$  in Eqs. (18) and (25) or Tables I and II<sup>2</sup>] was resolved into its components in the  $x$ ,  $y$ , and  $z$  directions. These resolved polarizations were denoted  $P_x$ ,  $P_y$ , and  $P_z$ ; in the models considered  $P_z$  was always zero. In the paper, the factors  $\sin\theta \sin\xi$  and  $\cos\theta \sin\xi$  in the expressions for  $P_x$  and  $P_y$  preceding Eqs. (26) and (35) should be omitted.

(2) Next, the average values of  $P_x$  and  $P_y$  were obtained for all possible orientations of the applied field. These averaged polarizations were denoted by  $\bar{P}_x$  and  $\bar{P}_y$  and are given by

$$\bar{P}_x = \langle P_x \cos\theta \sin\xi \rangle_{AV}$$

and

$$\bar{P}_y = \langle P_y \sin\theta \sin\xi \rangle_{AV}.$$

The averaging of  $P_x$  and  $P_y$  over all orientations of the field implies that the sample is polycrystalline. It should be noted that the field  $F$  used in the paper was  $F = F_0 \sin\xi$ , i.e.,  $F$  is the component of the field in the  $x$ – $y$  plane. This introduces a factor of  $\sin\xi$  in  $P_x$  and  $P_y$ . The latter quantities always involve a term in  $\sin\theta$  or  $\cos\theta$ , so one encounters the quantities  $\langle \sin^2\theta \sin^2\xi \rangle_{AV}$  or  $\langle \cos^2\theta \sin^2\xi \rangle_{AV}$  in calculating  $\bar{P}_x$  and  $\bar{P}_y$ . Both averages are readily shown to be  $\frac{1}{2}$ . The  $\sin^2\xi$  term in these averages was misprinted  $\sin\xi$  just after Eq. (26).

(3) The total polarization associated with mode 2 was then obtained using  $P_2 = \bar{P}_x + \bar{P}_y$ . Either  $\bar{P}_x$  or  $\bar{P}_y$  was zero for a given mode. The polarizability was obtained using  $\alpha_2 = P_2/NF_0$ . The polarizability for the other modes was calculated by an analogous procedure.

Calculations on several three-dimensional models with symmetrical spatial arrangement of the possible sites have been completed, and the results are qualitatively similar to those for a single-axis rotator. A distribution of dielectric relaxation times and a low polarizability appear when one site is more stable than the others, but only a single relaxation time with a polarizability of  $\mu_0^2/3kT$  is found when the sites are equivalent. Work has also been completed on a single-axis rotator with four rate constants.

<sup>1</sup> J. D. Hoffman and H. G. Pfeiffer, *J. Chem. Phys.* **22**, 132 (1954).

<sup>2</sup> It should be noted that Table II is for the  $C_{ij}$  for  $k' \gg k$  and not  $k' = k$ .

## Rare Gas Permeation through Polymers

FRANCIS J. NORTON

General Electric Research Laboratory, Schenectady, New York  
(Received April 12, 1954)

IN a study of gas permeation through solids, an unexpected result was obtained. It was found that the heavier rare gases may have a faster steady-state rate of permeation through some polymers than does helium.

The procedure for measuring rates of permeation was similar to that employed in the determination of helium diffusion through a variety of glasses.<sup>1</sup> The mass spectrometer was used to positively identify the gas and to measure its permeation rate through a 50-mil polymer sheet.

The permeation rate is given in units employed by Dushman<sup>2</sup> and Barrer,<sup>3</sup> that is, in cubic centimeters of gas at normal temperature and pressure (760 mm Hg, 0°C) per second per cm<sup>2</sup> area per millimeter thickness per cm Hg gas differential, partial pressure.

At 25°C, the following rates of permeation were found.

	Xenon	Helium
Perbunan	$8 \times 10^{-10}$	$38 \times 10^{-10}$
Butyl rubber	$11 \times 10^{-10}$	$40 \times 10^{-10}$
Neoprene	$100 \times 10^{-10}$	$45 \times 10^{-10}$
Natural rubber	$430 \times 10^{-10}$	$230 \times 10^{-10}$

The explanation probably lies in the balance between the two factors for permeation: solubility and internal diffusion. One would expect the diffusion to be faster for the smaller atom. However, in some cases, as for water, xenon solubility is higher than helium solubility.<sup>4</sup> High solubility is also often accompanied by high permeability. So here, the high permeability for natural rubber would probably be accompanied by high solubility for xenon. This is related to the fact that long times, often several days, were required to establish steady-state flow rates for xenon at 25°C, and long periods were subsequently needed to degas the 50-mil membrane free of xenon. Where the permeation rate is low, as xenon through perbunan, the diffusion factor predominates over the solubility factor.

<sup>1</sup> F. J. Norton, *J. Am. Ceramic Soc.* **36**, 90-96 (1953).

<sup>2</sup> S. Dushman, *Scientific Foundations of Vacuum Technique* (John Wiley and Sons, Inc., New York, 1949).

<sup>3</sup> R. M. Barrer, *Diffusion In and Through Solids* (Macmillan Company, New York, 1941).

<sup>4</sup> E. Lange and R. Watzel, *Z. physik. Chem. (A)* **181**, 1 (1938).

## Erratum: Flame Zone Studies by the Particle Track Technique. I. Apparatus and Technique

[*J. Chem. Phys.* **22**, 106 (1954)]

R. M. FRISTROM, W. H. AVERY, R. PRESCOTT, AND A. MATTUCK  
Applied Physics Laboratory, The Johns Hopkins University,  
Silver Spring, Maryland

THE last term in Eq. (2), page 107, was inverted. The equation should read

$$T_1 = T_0 [v_i/v_0] [r_i/r_0] [M_i/M_0]. \quad (2)$$

The authors are indebted to Mr. E. E. Frost for bringing this error to our attention.

## The Anomalous Magnetic Behavior of $UI_3$ from 1-4.2°K

L. D. ROBERTS AND D. E. LAVALLE,

Oak Ridge National Laboratory, Oak Ridge, Tennessee

AND

R. A. ERICKSON, *University of Tennessee, Knoxville, Tennessee*

(Received April 12, 1954)

MEASUREMENTS<sup>1</sup> by J. K. Dawson have shown that the magnetic susceptibility of  $UI_3$  follows a Curie-Weiss law in the temperature region 200°K-394°K with a Weiss constant of 5°K. The small value of the Weiss constant suggested the possibility of a magnetic transition in the liquid helium temperature region. We have measured the differential magnetic susceptibility at 500 cycles on two 10-gram powder  $UI_3$  samples using a cryostat and mutual inductance bridge described elsewhere.<sup>2</sup> Figures 1 and 2 give plots of the reactive component  $\chi'$

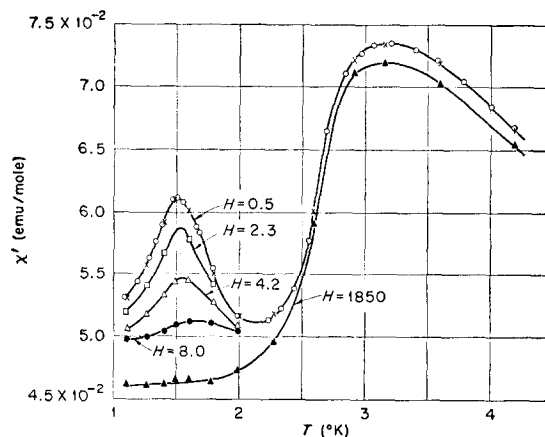


FIG. 1. Reactive component of the magnetic susceptibility of  $UI_3$  as a function of temperature and magnetic field— $H$  is in gauss.

and the resistive component  $\chi''$  of the susceptibility as a function of temperature and magnetic field. The maximum in  $\chi'$  at 3.20°K is interpreted to be an antiferromagnetic transition. In this temperature region  $\chi''$  remains very small, and both components of the susceptibility are found to be insensitive to the magnetic field up to 500 gauss. The peak at 1.50°K in  $\chi'$  is quite different from that at the Néel temperature. In this region the loss component  $\chi''$  rises sharply to a maximum at 1.38°K and both components are remarkably sensitive to a static magnetic field which is applied with a solenoid magnet mounted coaxially with the susceptibility measuring coils.<sup>2</sup> Both  $\chi'$  and  $\chi''$  are found to decrease almost linearly with increasing field up to about 5 oersted and this decrease appears to saturate at 300 to 500 gauss. These phenomena were observed to be virtually independent of frequency and amplitude of the oscillating field up to 1000 cycles and 3 oersted.

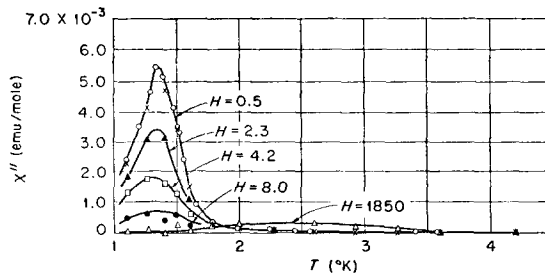


FIG. 2. Resistive component of the magnetic susceptibility of  $UI_3$  as a function of temperature and magnetic field— $H$  is in gauss.